

# Production of $\tau\tau jj$ final states at the LHC and the TauSpinner algorithm: the spin-2 case

M. Bahmani<sup>1</sup>, J. Kalinowski<sup>2</sup>, W. Kotlarski<sup>2,3</sup>, E. Richter-Was<sup>4</sup>, and Z. Was<sup>1,a</sup>

<sup>1</sup> Institute of Nuclear Physics, PAN, Kraków, ul. Radzikowskiego 152, Poland

<sup>2</sup> Faculty of Physics, University of Warsaw, Pasteura 5, 02-093 Warsaw, Poland

<sup>3</sup> IKTP, Technische Universität Dresden, Zellescher Weg 19, 01069 Dresden, Germany

<sup>4</sup> Institute of Physics, Jagellonian University, Łojasiewicza 11, 30-348 Cracow, Poland

the date of receipt and acceptance should be inserted later

**Abstract** The **TauSpinner** algorithm is a tool that allows to modify the physics model of the Monte Carlo generated samples due to the changed assumptions of event production dynamics, but without the need of re-generating events. With the help of weights  $\tau$ -lepton production or decay processes can be modified accordingly to a new physics model. In a recent paper a new version **TauSpinner ver.2.0.0** has been presented which includes a provision for introducing non-standard states and couplings and study their effects in the vector-boson-fusion processes by exploiting the spin correlations of  $\tau$ -lepton pair decay products in processes where final states include also two hard jets. In the present paper we document how this can be achieved taking as an example the non-standard spin-2 state that couples to Standard Model particles and tree-level matrix elements with complete helicity information included for the parton-parton scattering amplitudes into a  $\tau$ -lepton pair and two outgoing partons. This implementation is prepared as the external (user provided) routine for the **TauSpinner** algorithm. It exploits amplitudes generated by **MadGraph5** and adopted to the **TauSpinner** algorithm format. Consistency tests of the implemented matrix elements, reweighting algorithm and numerical results for observables sensitive to  $\tau$  polarization are presented.

**PACS.** 12.60.Fr, 07.05.Tp

## 1 Introduction

With increasing statistics collected by the LHC experiments the interests to explore final states with  $\tau$ -leptons gain importance. Because of the high mass and their decays,  $\tau$ -leptons may provide a sensitive window to physics beyond the Standard Model predictions. The **TauSpinner** algorithm, started with Ref. [1], provides a powerful tool to investigate characteristics of final states with  $\tau$ -leptons due to modifications in underlying physics models. This is obtained with the help of weights attributed to each event from collision data or Monte Carlo generated, and thus without repeating the detector response simulation with each variant of the physics model. An approach where physics assumption variation can be introduced with weights is useful for many modern data analysis techniques. The first version of **TauSpinner** reweighting found its application in the domain of Standard Model measurements [2] but also for New Physics limits established for simple  $2 \rightarrow 2$  parton level processes [3]. Later, in [4, 5], **TauSpinner** was found useful for discussion of CP sensitive massively multi-dimensional observables in

the frame of Machine Learning techniques [6]. In a recent paper [7] an extended version of **TauSpinner 2.0.0** was presented which now includes hard processes featuring tree-level parton matrix elements for production of a  $\tau$ -lepton pair and two jets. It was prepared as a tool to be helpful for studying spin effects in processes of Standard Model and searches of New Physics, like in Refs. [8, 9]. It found also tempting applications in the domain of implementation and discussion of variants for Standard Model electroweak calculation schemes used in simulation programs [7], and in experimental applications for Standard Model measurements [10–13].

Before discussing **TauSpinner** as a tool for studying observables of New Physics let us briefly recall some virtues of the **TauSpinner** algorithm. Since  $\tau$ -leptons cannot be observed directly due to their short life-time with more than 20 different decay channels, each with somewhat distinct signature, recalculating and reanalyzing observables involving  $\tau$  decays is time consuming. However the  $\tau$ -lepton spin polarization can be inferred from their decays, contrary to the case of electron or muon signatures. Spin effects can provide a better insight into the nature of the underlying physics. Therefore efforts to explore these phenomena are worth pursuing. **TauSpinner** allows to greatly

<sup>a</sup> e-mail: Z.Was@cern.ch

simplify the task of exploring the experiments' sensitivity. Evaluation of measurements significance due to different New Physics models can be performed with the help of event weights. Technical aspects of the algorithm in case of configurations with two jets accompanying a  $\tau$ -lepton pair have been covered in [7].

The purpose of the present paper is to document how the user can apply the **TauSpinner** algorithm to his/her physics model. To this end, we take as a case study a non-standard spin-2 object coupled to SM particles. We analyze its production in proton-proton collisions and decay to a  $\tau$ -lepton pair, addressing also the question to what extent  $\tau$  polarization can be exploited to investigate its nature. We demonstrate how **TauSpinner** can facilitate such studies with the help of matrix elements for that model (or any other, provided by the user). Corresponding weight can be calculated and applied to each event of samples with full experiment simulation chains. As it is practically impossible to repeat simulations with detector response effects included for each new physics hypothesis, our procedure is beneficial and may be the only available option for the general use despite its limitations. **TauSpinner** algorithm can also be applied on measured data events, e.g. in the context of embedded  $\tau$  lepton techniques [14].

The paper is organized as follows: Section 2 and Appendix A provide details of **TauSpinner** which were not discussed in Ref. [7], or treated very briefly, but are of importance for the case of New Physics models. Section 3 documents details of the tree-level matrix elements used for the calculation of spin-2 object exchange amplitudes which are later passed for weights calculation in  $pp \rightarrow \tau\tau jj$  events. The implemented functionality is based on automatically produced FORTRAN code from **MadGraph5** package [15] similarly as for processes of the Drell-Yan-type and of the Standard Model Higgs boson production in vector-boson-fusion processes (VBF). We explain details of the modification which we have introduced to the code of amplitudes generated with **MadGraph5** (version MG5\_aMC\_v2.4.3). Section 4 and Appendix B are devoted to numerical results. First, tests for fixed kinematic configurations are recalled. Later, definitions of observables are given, and some distributions are presented. In Section 5 numerical results sensitive to  $\tau$  polarization are presented taking the single-prong decay  $\tau^\pm \rightarrow \pi^\pm \nu$  channel as a spin analyser. Section 6 summarizes and concludes the paper.

## 2 The **TauSpinner** weight $wt_{prod}^{A \rightarrow B}$

**TauSpinner** does not provide methods to generate  $pp$  collision events. Therefore, the necessary input for **TauSpinner** consists of a series of events, which could be of a process different than the required one but with the same outgoing final states. The events must contain information on the four momenta of (two) outgoing jets and  $\tau$ -leptons with their decay products, which is necessary for the calculation of the hard process matrix elements. Flavours of incoming/outgoing partons are determined by the algorithm -

there is no need to read them from the generated events. The sum over all possible configurations, weighted with PDFs, is performed. On the other hand, the information on the decay products of  $\tau$ -leptons is needed for the evaluation of spin effects. Using this input, the value of the corresponding matrix elements can be calculated on the event by event basis and in particular the corresponding spin weight. As discussed in detail in Ref. [7], for each event

$$j_i(p_1)j_j(p_2) \rightarrow j_k(p_3)j_l(p_4)\tau^+\tau^-, \quad (1)$$

where  $j$  stands for a quark, antiquark or a gluon, the algorithm calculates the weight

$$wt_{prod}^{A \rightarrow B} = \frac{\sum_{ijkl} \frac{1}{\Phi_{flux}^{i,j}} f_i^B(x_1) f_j^B(x_2) |M_{ijkl}^B(\{p\})|^2 d\Omega(\{p\})}{\sum_{ijkl} \frac{1}{\Phi_{flux}^{i,j}} f_i^A(x_1) f_j^A(x_2) |M_{ijkl}^A(\{p\})|^2 d\Omega(\{p\})} \quad (2)$$

which represents, for a given phase-space point ( $\{p\}$ ) = ( $p_1, p_2, p_3, p_4, p_{\tau^+}, p_{\tau^-}$ ), the ratio due to the matrix element used in the generation of the sample for process (A) and the matrix elements corresponding to a New Physics model<sup>1</sup> (B). The evaluation of the weight in Eq. (2) requires the knowledge of contributions from all possible parton level configurations ( $ijkl$ ) weighted with parton density functions  $f_{i/j}^{A/B}(x)$  and flux factors  $\Phi_{flux}^{i,j}$ . The sums run over both gluons and quark flavours alike. Note however, that the flavour is passed to the user provided matrix element routine and flavour dependence can be introduced there. For the details and explanation of a notation used in formula (2) we refer to [7]. For the purpose of calculating  $wt_{prod}^{A \rightarrow B}$  we sum over all possible helicity configurations of outgoing  $\tau$ -leptons. An event generated for the process (A), when weighted with  $wt_{prod}^{A \rightarrow B}$  becomes an event of the process (B). Spin effects in  $\tau$  decays have to be introduced separately, with **TauSpinner** main spin weight  $WT$ , as explained in Appendix A.

The following details need to be stressed when selecting a suitable process (A) given the target process (B). For the narrow resonance, like the Higgs state, the value of matrix elements vary greatly with the invariants built from the final state four-momenta. Therefore the numerical stability needs to be kept in mind. The **TauSpinner** algorithm must reconstruct invariant mass of the resonance with the precision better than 1-2 MeV from the four-momenta of final state particles, whose energies may lie in the range of TeV. Double precision may be needed since otherwise some invariants may be inappropriately evaluated due to simple computer rounding errors. A user has to assure that the reweighting indeed works in the interesting regions of the phase-space. In particular, that the phase-space is populated for both processes (A) and (B) with not too massively distinct distributions, and that the distribution enhancements due to intermediate resonances or collinear or soft singularities have similar (matching) structure. Listed above checks require the hard processes information only.

<sup>1</sup> It can be also a variant of the Standard Model initialization, e.g. distinct electroweak schemes.

### 3 New Physics model of $(2 \rightarrow 4)$ process

As a case study we consider a simplified model of a massive gauge singlet spin-2 object  $X$  coupled to the SM gauge bosons. We use this model to demonstrate how to prepare and test external matrix element to be used by **TauSpinner** algorithm.

Scenarios with spin-2 objects have been already intensively studied in the literature in the context of LHC phenomenology [17–19], though none of the studies was dedicated to the analysis of  $X$  decays into  $\tau$  final states. Note however that for a general study of a "Higgs"-like resonance and its parity in vector-boson-fusion processes with a  $\tau$  pair as a decay product, experimental results are becoming available [20, 21].

In Ref. [3] we studied a Drell-Yan-like production of  $\tau$ 's through a hypothetical spin-2 object  $X$ . Building on our previous work, we study now the  $X$  production in the VBF topology, followed by  $X \rightarrow \tau^+\tau^-$  decay. We start by extending the Lagrangian of Ref. [3] by a set of gauge invariant dimension 5 operators, coupling the field  $X$  to gauge boson field strength tensors  $B$ ,  $W$  and  $G$  as

$$\mathcal{L} \ni \frac{1}{F} X_{\mu\nu} (g_{XBB} B^{\mu\rho} B_{\rho}^{\nu} + g_{XWW} W^{\mu\rho} W_{\rho}^{\nu} + g_{Xgg} G^{\mu\rho} G_{\rho}^{\nu}), \quad (3)$$

where group indices are implicitly summed over (where appropriate). The parameter  $F$ , set to 1 TeV, is introduced to keep the coupling constants dimensionless. Note that we are agnostic on the origin of the state  $X$ , in particular we do not claim it is connected to gravity. Hence we do not couple it to the entire energy momentum tensor and couplings  $g_X$  are kept as free parameters. This is in contrast to, for example Ref. [22], where the  $X$  field is coupled to the energy momentum tensor of quantized SM.

After the electroweak symmetry breaking, operators in Eq. (3) generate vertices with couplings of  $X$  to photons,  $W^{\pm}$ 's,  $Z$ 's and gluons; the explicit formulas for those couplings can be found in [19]. Since in this work we focus on technical aspects of incorporating the couplings of  $X$  to the EW gauge bosons, for numerical tests of the correctness of the Matrix Element implementation, we set  $g_{XBB} = g_{Xgg} = 0$ . Relevant diagram topologies are shown in Fig. 1: for the VBF process (Fig. 1a) and the  $X$ -strahlung process (Fig. 1b).

#### 3.1 Generating matrix-element code using MadGraph5

The extension of the SM by spin-2 field coupled to the gauge fields as in Eq. (3), including also coupling of the  $X$  field to quarks and  $\tau$ -leptons from [3], is encoded into a **FeynRules** [23] model. The **FeynRules** model file, together with its **UFO** output [24], is available in supplementary materials of the arXiv version of this reference. The **UFO** model is used to generate squared matrix elements using **MadGraph5**, employing the spin-2 support of the **HELAS** library [25]. This is done with the following set of commands

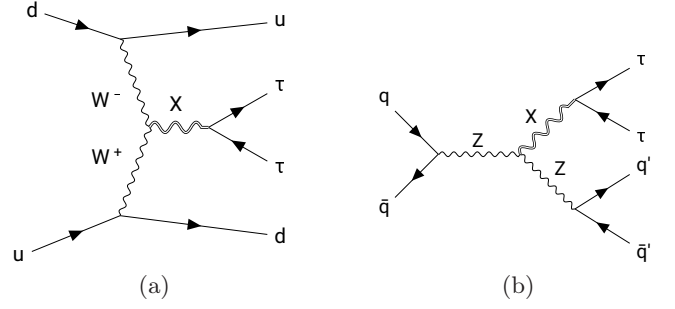


**Figure 1.** Topologies of Feynman diagrams for  $X$  production through its coupling to gauge bosons. Similar diagrams, with different combinations of  $W^{\pm}$ 's,  $Z$ 's, photons and quark flavours also exist.

- (a) `import model spin2_w_CKM_UFO`
- (b) by default, "multiparticles" containers already include all massless partons  
`p = g u c d s u~ c~ d~ s~`  
`j = g u c d s u~ c~ d~ s~`
- (c) generate spin 2 matrix elements  
`generate p p > j j x QED<=99 QCD<=99`  
`NPgg<=99 NPqq<=99 NPVV<=99, x > ta+ ta-`
- (d) write the output to disk in MadGraph's standalone mode using  
`output standalone "directory name"`

`NPgg`, `NPqq` and `NPVV` parameters control the maximum number of  $g_{Xgg}$ ,  $g_{Xq\bar{q}}$  and  $g_{XWW}$ ,  $g_{XBB}$  couplings, respectively. Limiting them by 99 effectively means that their number is not restricted. The model includes the CKM matrix in the Wolfenstein parametrization. As was stated above, for numerical tests we restrict ourselves setting  $g_{XBB} = g_{Xgg} = 0$ , though we stress again that the matrix element, coded as an example user process, contains all of them, see Appendix B for actual initialization of coupling constants.

#### 3.2 Integrating matrix-element code into TauSpinner example

The matrix element code is based on automatically produced **FORTRAN** subroutines by **MadGraph5** package, similarly as it has been done for processes of the Drell-Yan-type and of the Standard Model Higgs boson production in vector-boson-fusion (VBF)/Higgs-strahlung processes [7]. In the spin-2 case they have been also manually modified and adapted to avoid name clashes. This technical complication is a consequence of the fact that C++ user function for the spin-2 matrix element calls **FORTRAN** code created by **MadGraph5**. We therefore can not profit from **namespace** functionality of C++ as a natural solution to this problem. Some name changes are necessary, as explained below. The corresponding code is stored in the directory **TauSpinner/examples/example-VBF/SPIN2/ME**.

The generated codes for the individual sub-processes are grouped together into subroutines, depending on the flavour of initial state partons, and named accordingly. For example,

**Table 1.** List of implemented processes contributing to the spin-2  $X$  particle production, grouped into categories which differ by flavours of incoming partons. For each category, the names of **FORTTRAN** files calculating squared matrix elements, for given flavour configuration of incoming partons, are given in the second column. Examples of processes in each category are given in the last column.

Category of Matrix Elements	Corresponding <b>FORTTRAN</b> files	Processes
(1)	<i>GG_S2.f</i>	$gg \rightarrow \sum_f q_f \bar{q}_f X$
(2)	<i>GC_S2.f, GU_S2.f</i>	$gq_f \rightarrow gq_f X$
(3)	<i>GCX_S2.f, GUX_S2.f</i>	$g\bar{q}_f \rightarrow g\bar{q}_f X$
(4)	<i>DD_S2.f, UD_S2.f, UU_S2.f, CC_S2.f, CS_S2.f, SS_S2.f, CD_S2.f, CU_S2.f, SD_S2.f, SU_S2.f</i>	$q_{f_1} q_{f_2} (\bar{q}_{f_1} \bar{q}_{f_2}) \rightarrow q_{f_1} q_{f_2} (\bar{q}_{f_1} \bar{q}_{f_2}) X$
(5)	<i>DDX_S2.f, UDX_S2.f, UUX_S2.f, CCX_S2.f, CSX_S2.f, DCX_S2.f, SCX_S2.f, SSX_S2.f, UCX_S2.f, CDX_S2.f, CUX_S2.f, SDX_S2.f, SUX_S2.f</i>	$q_{f_1} \bar{q}_{f_2} (\bar{q}_{f_1} \bar{q}_{f_2}) \rightarrow q_{f_1} \bar{q}_{f_2} (\bar{q}_{f_1} \bar{q}_{f_2}) X$ $q_{f_1} \bar{q}_{f_2} (\bar{q}_{f_1} \bar{q}_{f_2}) \rightarrow gg X$

#### SUBROUTINE DCX\_S2(P,I3,I4,H1,H2,ANS)

encompasses the  $X$  production processes initiated by the  $d\bar{c}$  partons. We follow our previous convention [7] where symbol  $X$  in the subroutine or internal function name after the letter **U,D,S** or **C** means that the corresponding parton is an antiquark, i.e. **UXCX** corresponds to processes initiated by  $u\bar{c}$  partons, while **GUX** to processes initiated<sup>2</sup> by  $g\bar{u}$ . The **S2** stands explicitly for the production of spin-2  $X$  state. The input variables are: real matrix **P(0:3,6)** for four-momenta of incoming and outgoing particles, integers **I3,I4** for the Particle Data Group (PDG) identifiers for final state parton flavours and integers **H1,H2** for the outgoing  $\tau$  helicity states. Before integrating these subroutines into the **TauSpinner** program, a number of modifications have been done for the following reasons:

- Since **MadGraph5** by default sums and averages over spins of incoming and outgoing particles, while we are interested in  $\tau$  spin states, the generated codes have to be modified to keep track of the  $\tau$  polarization, i.e. indices/helicities **H1** and **H2**.
- Moreover, since the subroutines and internal functions generated by **MadGraph5** have the same names for all sub-processes, namely **SMATRIX(P,ANS)**, the names had to be changed to be unique. As an example, the subroutine name for the subprocess  $u\bar{d} \rightarrow c\bar{d} X$ ,  $X \rightarrow \tau^+ \tau^-$  was changed to **UDX\_CDX\_S2(P,H1,H2,ANS)**. These subroutines will be called by subroutine **UDX\_S2(P,4,-1,H1,H2,ANS)**.
- For a pair of final-state parton flavours  $k \neq l$ , the **MadGraph5** generated codes have been obtained for a definite ordering  $(k,l)$ , but not for  $(l,k)$ , to reduce the number of generated configurations. When **TauSpinner** is invoked, the configuration of outgoing

partons is unknown and it takes into account both possibilities: thus a compensating factor  $\frac{1+\delta_{l,k}}{2}$  has to be introduced due to the way of organizing the sum in Eq. (2) and in Ref. [7].

- For calculation of matrix elements **MadGraph5** is using **ALOHA** functions [26] stored in **FORTTRAN** subroutines. Since some of these functions have originally names identical to functions in the **TauSpinner** source code for the implementation of the Standard Model VBF/Higgs-strahlung production, names of those functions have to be modified also to avoid any name conflicts. Therefore **ALOHA** functions stored in **TauSpinner/examples/example-VBF/SPIN2/ME/Spin2\_functions.f** are changed by adding "\_S" suffix to the original names of subroutines, for example **FFV4\_0** is changed to **FFV4\_0\_S**.

Table 1 summarizes the naming convention for the files. At the parton level each of the incoming or outgoing partons can be one of the flavours:  $\bar{c} \bar{s} \bar{u} \bar{d} g d u s c$ , with Particle Data Group (PDG) identifiers: -4, -3, -2, -1, 21, 1, 2, 3, 4 respectively. For processes with two incoming partons, two outgoing  $\tau$ -leptons and two outgoing partons, there are  $9^4$  possibilities, most of them evaluating to 0 or obtainable one from another, by relations following from CP symmetries and/or permutations of incoming and/or outgoing partons.

For each point in the parton level phase-space, consisting of all incoming and outgoing four momenta as well as their flavours, depending on the user choice, one of two variants of processes (i.e. pairs of matrix elements) may be used by **TauSpinner** executable. That is: the Drell-Yan variant (standard, and user provided New Physics matrix

<sup>2</sup>  $X$  in this context should not be confused with the spin-2 field  $X$ .



elements) or Higgs-like variant (again standard, and user provided one<sup>3</sup>).

Certain limitations need to be kept in mind. In practice, it is simply impossible to obtain statistically significant distribution of weighted events for the particular model under study in the region of phase-space where original sample is sparse or possibly no events are present at all. In particular, the mass and width of the Higgs-like resonance need to coincide (be close) to those of the Higgs. Also, the algorithm is expected to be used in regions of the phase-space where kinematic distributions of the original and New Physics models are not massively different.

## 4 Tests of implementation of external matrix elements

Once the user-provided external matrix elements are prepared, numerical tests are necessary if it indeed has been implemented properly into the TauSpinner environment. In the following we discuss such tests, using spin-2 matrix elements of  $Xjj$  production as an example. We start from the technical one and continue with more physics oriented ones. Finally we will demonstrate limitations of the method.

### 4.1 Test of matrix elements using fixed kinematic configuration

For checking the consistency of the implemented codes generated with MadGraph5 and modified as explained in section 3.2, we have chosen a single event with fixed kinematic configuration at the parton level. We have calculated the matrix elements squared for that event and for all possible helicity and parton flavour configurations, using the code implemented as user example. We compared results with the numerical values obtained directly from MadGraph5. The agreement of at least 6 significant digits has been confirmed.

### 4.2 Tests of matrix elements using series of generated events

As further tests of the internal consistency of external matrix element implementation, we have explored the reweighting procedure by comparing a number of kinematic distributions obtained directly or reweighted with  $wt_{prod}^{A \rightarrow B}$  from series of 10M events generated by MadGraph5 for  $X$  particle and Higgs boson. Samples were generated for pp collisions at 13 TeV using CTEQ6L1 PDFs. The mass of both  $X$  particle and Higgs boson was set to 125 GeV and the width to 5.75 MeV. The details of cuts and MadGraph5 initialization used for the sample generation are given in Ref. [16]. On the generated events the following further selections were applied:  $m_{jj\tau\tau} < 1500$  GeV,  $p_T^{\tau\tau} < 600$  GeV

<sup>3</sup> The prototype is implemented in the example, see Appendix A.1.

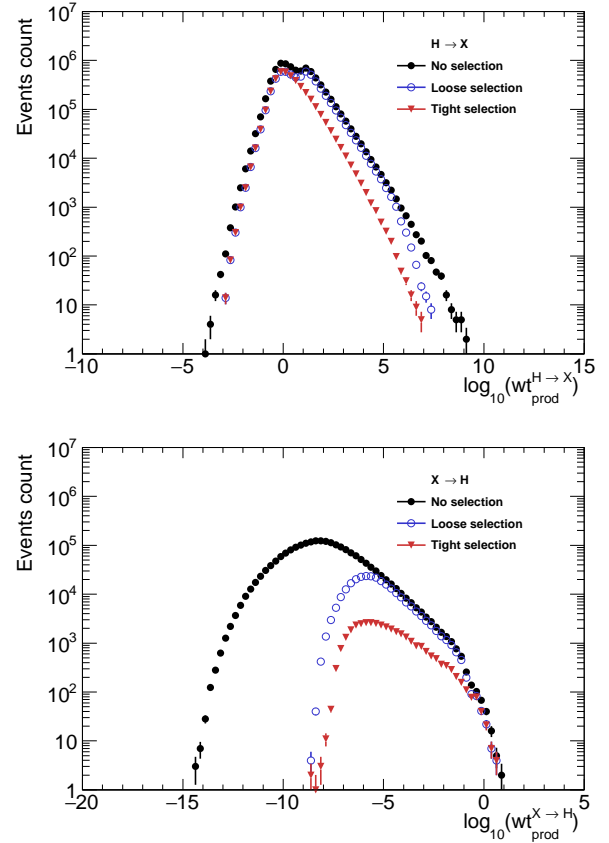


**Figure 2.** Weight distribution for  $H$  sample reweighted to  $X$  (top panel) and for the  $X$  sample reweighted to  $H$  (bottom panel). If the distribution featured a long tail extending to high weights, it would indicate a problem with reweighting in regions of the phase-space where the ratio of the matrix element (B) with respect of the one of the original sample (A) is too large in comparison to the typical event.

and  $m_{jj} < 800$  GeV (loose selection) to eliminate excessive weight regions of the phase space, or eliminating also  $Z \rightarrow jj$  or  $W \rightarrow jj$  resonance peaks  $100 < m_{jj} < 800$  GeV (tight selection).

Before commenting on the actual results let us point to the size of statistical errors<sup>4</sup> which reflect comparability of the  $H$  (process A) and  $X$  (process B) samples. Errors are always larger than what could be expected from weight-one samples of the similar size. This effect can be understood better with the weight distributions shown in Fig. 2. In both cases of reweighting: from  $H$  to  $X$  (top panel) and  $X$  to  $H$  (bottom panel), one can observe a constant slope on this double logarithmic plot with clear sharp upper end. With such spectrum of weights statistically sensible calculation of the cross sections and distributions may be still possible. If a tail of events with

<sup>4</sup> The statistical errors of all histograms, including the ones using weighted events, were evaluated by the standard algorithms of the root library [27].

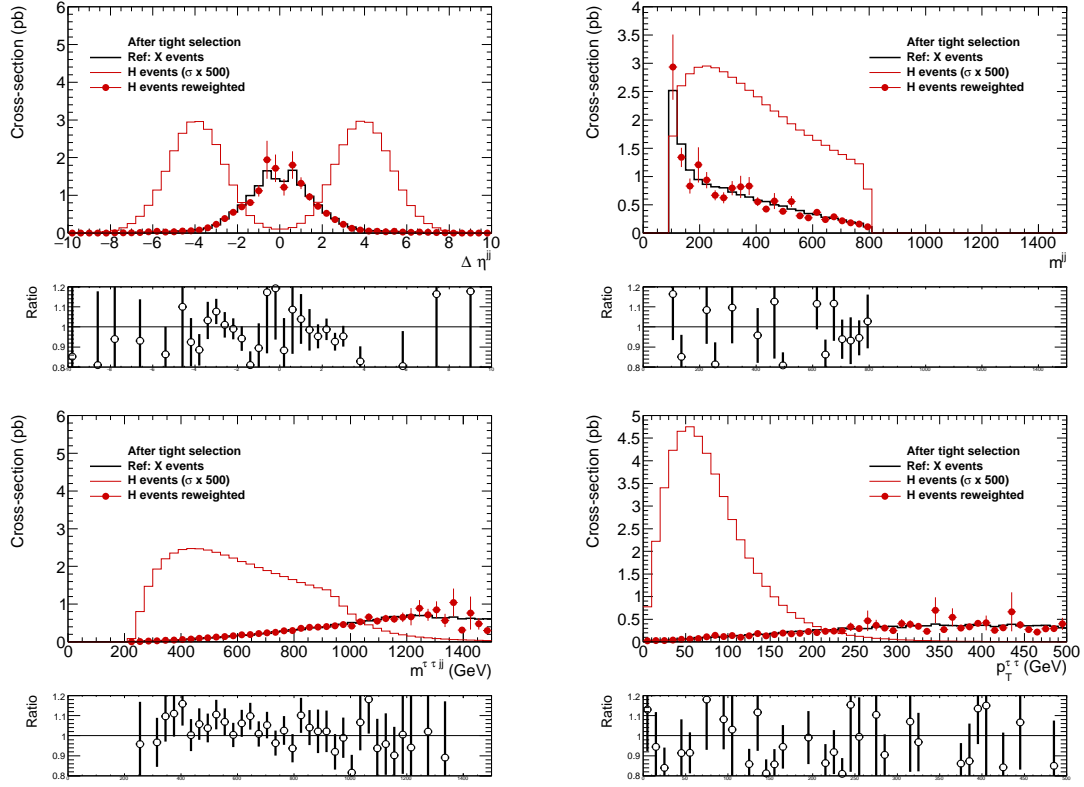


**Figure 3.** The  $H$  sample reweighted to the  $X$  and compared with the  $X$  sample. The  $H$  and  $X$  widths are of 5.75 MeV. Selection cuts: Invariant mass of outgoing particles  $m^{\tau\tau jj} < 1500$  GeV, invariant mass of jets system  $100 < m^{jj} < 800$  GeV and  $p_T^{\tau\tau} < 600$  GeV. Variables on the x-axes as explained in Section 4.2.

**Table 2.** Cross sections for the generated  $H$  production process and after its reweighting to the  $X$  production ( $H \rightarrow \tau\tau$  block), and for the generated  $X$  production and after its reweighting to  $H$  production ( $X \rightarrow \tau\tau$  block); acceptances with no, loose or tight selections applied for generated and reweighted event samples are also shown.

Events		No selection	Loose selection	Tight selection
$H \rightarrow \tau\tau$	Acceptance	100%	73.8%	49.0%
	$\sigma$ [pb] (H)	$[2.033 \pm 0.064] 10^{-1}$	$[1.501 \pm 0.062] 10^{-1}$	$[1.004 \pm 0.045] 10^{-1}$
	$\sigma$ [pb] ( $H \rightarrow X$ )	$[9.097 \pm 1.270] 10^{+2}$	$[1.187 \pm 0.038] 10^{+2}$	$[1.517 \pm 0.066] 10^{+1}$
$X \rightarrow \tau\tau$	Acceptance	100%	13.0%	1.71%
	$\sigma$ [pb] (X)	$[9.097 \pm 0.0029] 10^{+2}$	$[1.178 \pm 0.001] 10^{+2}$	$[1.544 \pm 0.004] 10^{+1}$
	$\sigma$ [pb] ( $X \rightarrow H$ )	$[2.023 \pm 0.0474] 10^{-1}$	$[1.478 \pm 0.031] 10^{-1}$	$[9.75 \pm 0.309] 10^{-2}$

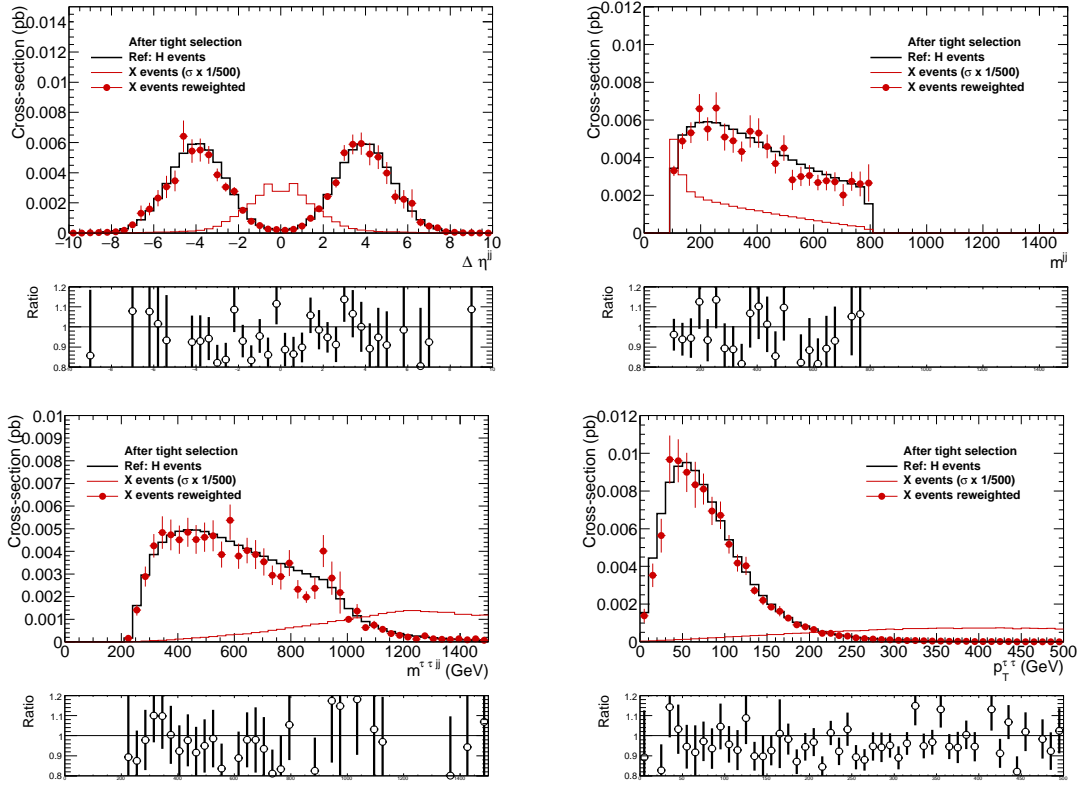


**Figure 4.** The  $X$  sample reweighted to the  $H$  and compared with the  $H$  sample. The  $H$  and  $X$  widths are of 5.75 MeV. Selection cuts: invariant mass of outgoing particles  $m^{\tau\tau jj} < 1500$  GeV, invariant mass of jets system  $100 < m^{jj} < 800$  GeV and  $p_T^{\tau\tau} < 600$  GeV. Note that statistical errors for the distributions obtained with reweighting (red points) are much larger than for the case of Fig. 3. This is predominantly due to small acceptance of  $X$  sample: 1.7% only. But the agreement with the reference distribution (black histogram) remains within statistical fluctuation (dominated by large weight events). Variables on the x-axes as explained in Section 4.2.

ever higher weights would continue to form when increasing size of samples, statistical errors would never decrease. This happens, for example, if in some sub-dimensional-manifold of the phase space the matrix element has a zero. Then with increasing statistics, events closer and closer to this zero are generated, and feature larger and larger weights. Even though contribution of such events to the weighted distribution is formally finite and integrable, the error estimate of the Monte Carlo generated distribution will not get reduced with the increasing statistical sample.

The tests were performed on a set of kinematic distributions: pseudorapidity of outgoing parton  $j$ , rapidity of  $\tau\tau$  and  $jj$  systems, invariant mass of  $\tau\tau$  system, pseudorapidity of  $\tau\tau$  system, opening angle between jets, opening angle between  $\tau$ 's, angle between incoming parton and outgoing parton in the rest frame of jets and angle between resonance and outgoing parton in the rest frame of jets.

Plots for all these variables can be found on the web page [16]. Here, in Fig. 3 and Fig. 4, we present only plots for: the difference of jet's rapidities  $\Delta\eta^{jj}$ , the invariant mass of the jet pair  $m^{jj}$ , the transverse momentum of  $\tau$  pair  $p_T^{\tau\tau}$  and finally the invariant mass of  $\tau$ -pair and jet-pair combined  $m^{\tau\tau jj}$ . In each plot the distribution **Ref**, for the reference process, is shown as a black histogram while the red histogram is the original distribution of generated events which are reweighted using **TauSpinner**  $wt_{prod}^{A \rightarrow B}$  weight to obtain the distribution represented by the red points with error bars. For the test to be successful, the red points should follow the black histogram; the ratio of **Ref** and reweighted distributions is shown in the bottom panel of each figure.

In both Figs. 3 and 4, the reweighted distributions follow the **Ref** histograms. When reweighting of  $X$  to  $H$  (see Fig. 4), the distributions feature larger statistical errors than in the case of  $H$  to  $X$  reweighting (Fig. 3). This is simply because tight selection cuts leave only 1.7% of  $X$  events due to eliminating configurations with small  $m_{jj}$ . For some bins the reweighted distribution lies below target (black) distribution, whereas the ones with big errors tend to lie above. If similar feature appears when sample size is increased it points to the possibility that original distribution had a zero along some hyperspace. Nevertheless, if in distributions normalized to cross section the neighbouring bins have no deficit of content, then the reweighting algorithm can be still used.

The tests validating reweighting algorithm are completed with the ones monitoring overall normalizations (integrated cross sections). For our samples and initializations, the resulting cross sections are shown in Table 2. Reasonable agreement between cross sections obtained from the **MadGraph5** calculation and with reweighting was obtained, see Table 2 where the first line in the  $H \rightarrow \tau\tau$  block should be compared to the second line in the  $X \rightarrow \tau\tau$  block and vice-versa. Such a study has to be repeated for each new matrix element implemented and whenever selection cuts are changed sizably.

### 4.3 On reliability of the **TauSpinner** reweighting approach

The **TauSpinner** reweighting method is atypical compared to methods used in other tools, like **REPOLO** [28] **PHYTIA** [29], **SHERPA**. [30] or **MadGraph** [31]. Let us explain what are the advantages and disadvantages behind such a choice.

The advantage of our method is that it does not assume any knowledge of the initial and outgoing partons and tau leptons beyond their four momenta. Therefore it can be applied directly to the experimental data, e.g. of the embedded  $\tau$  samples. We have demonstrated that our reweighting method is reliable for the hard process matrix elements convoluted with PDF's. The disadvantage is that it does not address the issue that both the parton shower and hadronization do depend on color configuration as well as on flavours of partons. Once event is reweighted, the reshuffle between categories of different color and/or flavour content takes place, inevitably leading to biases.

In experiment simulation production files [32] color information for the so called truth entries is not stored. Even in the data formats prepared and agreed on by the community [33], such information, at best, consists of a connected tree, navigation inside of which retains information on the event history including the parents of unstable particles. There is an important caveat here: the event generators are modeling quantum processes, and the event record has the structure of a classical decay chain. It is inevitable that compromises must be made and difficulties can arise from an over-literal interpretation of the tree structure. For the color it means that at best the so called flow approximation is pre-imposed. Even for such partial information, there are no detailed commonly accepted rules how it should be stored, see for example Section 2.3 in [34] or Section 4.4.1 in the **HepMC** manual [35] or [36].

In practice, in experiment production files of detector response simulated events, information on intermediate quantum states is generally not available. Usually only the 4-momenta of partons and their flavours are stored. We are not in a position to affect these experiments choices. Multitude of arguments have been raised for such choices, including the fact that distinct generators prepared by theorists, provide such information in different manner, or that it makes data files unnecessary large. We can only address the question if any useful solution for reweighting may be designed<sup>5</sup> and what kind of restrictions it implies have to be kept in mind.

There are two simulation steps which depend on hard process configurations of flavours and colors: parton shower and later hadronization. It is well known that even mainstream Monte Carlo programs do not match in this respect sufficiently well the experimental data for all

<sup>5</sup> Note that for spin effects we include in our re-weighting not only production matrix element, but the ones of  $\tau$ 's decays as well.



required phase space regions [37]. This is a complex issue which we can not exhaust<sup>6</sup>.

The discussion of the resulting systematic errors of our method is out of scope of the present paper. It would require evaluation of how mismatches of the color and flavour input for parton shower and hadronization translates into reconstructed jets from simulated detector responses. This in turn would require the use of experimental detector response codes, not available publicly. In general, the **TauSpinner** application domain is restricted to observables where details of jets, resulting from partons flavours or color are not of importance. This has to be kept in mind.

Let us point that our study examples of the previous sub-sections are for the cases, where starting and target distributions are massively different. In practical applications we expect **TauSpinner** to be used in configurations where new contributions to matrix elements are at the edge of observability.

If required, it is possible to apply **TauSpinner** in the flavour savvy manner. Possible solution may follow the method described in Appendix A. Contributions from distinct flavour configurations can be treated separately only for cases when in experiment production files the flavour configurations are stored, or can be unwinded.

## 5 Spin dependent characteristics

So far we were discussing observables relying on the kinematics of final states consisting of four momenta of  $\tau$  leptons and accompanying two jets. Inclusion of  $\tau$  decay products increase the phase space dimensionality substantially, making the analysis much more difficult, especially when dependence on selection cuts is taken into account (as observed in previous sub-sections).

In the following, we will present a few spin dependent results obtained for the  $H$  and  $X$  samples within the tight selection cuts. Using **TAUOLA ++** [40] we supplement these samples with  $\tau$  decays in the simplest possible mode  $\tau^\pm \rightarrow \pi^\pm \nu$  with no spin effects included. Spin effects are introduced with the help of **TauSpinner** weights, which are calculated according to the production and decay kinematics (see Refs. [1, 41] for the spin weight definition).

Figure 5 shows the spin weight histograms for the  $H$  and  $X$  samples. In both cases the spin weights are calculated first using the matrix element for  $X$  productions as described in Ref. [3], that is featuring effective Born  $2 \rightarrow 2$  kinematic (open red circles), and compared with the new calculation in which amplitudes featuring two jet kinematics are taken into account (blue full circle points)<sup>7</sup>. In both

cases the same  $X - \tau\tau$  couplings were used. As expected (see Eq. 8 from Ref. [1]), for the  $2 \rightarrow 2$  case the range of spin weights is limited to  $[0, 2]$  since in this process there are no couplings which could lead to individual  $\tau$  polarization. In the  $2 \rightarrow 4$  case the spin weight distribution exhibits a tail which extends beyond 2 and covers most of the allowed  $[0, 4]$  range. This is due to, e.g., the presence of the subprocess  $W^+W^- \rightarrow X \rightarrow \tau^+\tau^-$  in which  $W$ 's radiated off quarks are polarized which has impact on  $\tau$  polarization. The tail above 2, although not so much pronounced, will manifest itself in the distribution of  $\tau$  decay products.

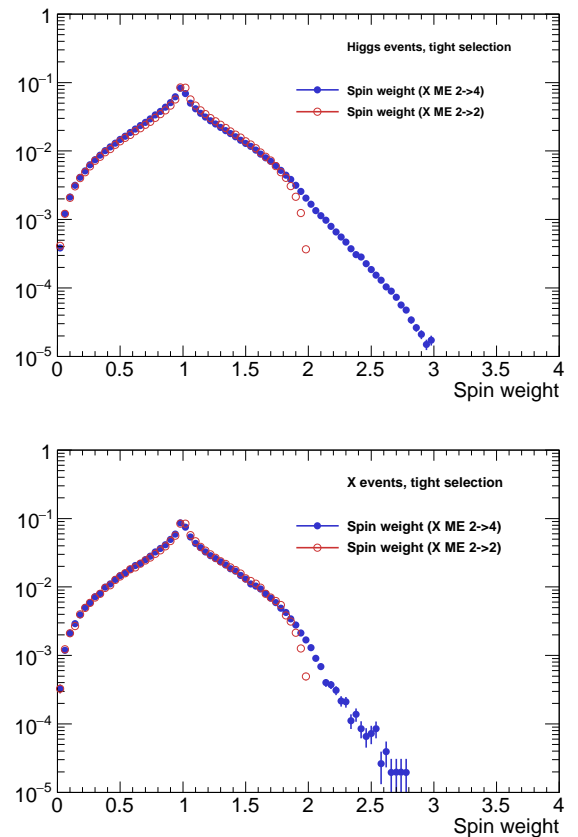


**Figure 5.** Spin weight histograms, normalized to unity, obtained from  $X$  matrix elements for  $H$  sample (top plot) and  $X$  sample (bottom plot). In both cases samples are constrained with tight selection cuts. Red open circles are when the effective Born ( $2 \rightarrow 2$ ) matrix elements are used and blue full circle points are when our new ( $2 \rightarrow 4$ ) matrix elements are used.

<sup>6</sup> Large effort is devoted to this aspect of phenomenology thanks to new data analysis techniques. For example, new interesting results are obtained thanks to Machine Learning approach [38, 39].

<sup>7</sup> Here we exploit the virtue of **TauSpinner** which allows, for a given sample, to calculate weights for different production mechanisms. This feature is of help in validating or rejecting theoretical hypotheses.

Let us now turn to the standard spin sensitive distribution of the ratio  $E_\pi/E_\tau$  (a fraction of  $\tau$  energy carried by the decay pion) used in [41] for benchmarking  $\tau$  polarization. In every case discussed below we will use again  $X$  production amplitudes to calculate  $\tau$  pair density mat-

rix. We will do that also for the sample generated with  $H$  production amplitudes<sup>8</sup>.

The  $\tau$  polarization can originate from the  $X$  production via VBF process, which is asymmetric over the phase-space regions due to the asymmetry of valence  $u$  and  $d$  quark distributions in the proton. To exhibit the polarization effects we have to sort out events according to the  $\tau$  polarization; otherwise the effects will average out. Since in the proton there are more  $u$ -type quarks than  $d$ -type, the  $X$  particle produced in the VBF preferentially will follow the direction of  $W^+$  which are right-handed and impart their polarization on  $X$  bosons. One can then expect that  $\tau$  lepton from  $X$  decay will have polarization dependent on  $\tau$  direction with respect to the  $X$  flight direction correlated with its spin polarization. Thus it is suggestive to sort events according to positive and negative value of  $C = Y_X \cdot (p_z^{\tau^-} - p_z^{\tau^+})$ , where  $Y_X$  denotes the  $\tau$  lepton pair rapidity and  $p_z^{\tau^-}$ ,  $p_z^{\tau^+}$  are the  $z$  components of  $\tau^\pm$  four-momenta. In Fig. 6 events with positive and negative  $C$  are plotted separately (the first bin for  $C > 0$  is lower exhibiting the pion mass  $m_\pi/m_\tau$  effect). We observe that spin weights, calculated with the  $X$  production amplitude, when applied to the  $H$  sample lead to a larger spin effect, than when applied to the  $X$  sample. In the second case the spin effect is barely visible<sup>9</sup>.

Our results illustrate the complexity of multidimensional distributions. Even within tight selection there is a sizable difference between events of  $X$  and  $H$  production, which is reflected in  $\tau$  polarization effects greater for the  $H$  sample than for  $X$  sample, even though the same  $pp \rightarrow \tau\tau jj$  matrix elements featuring intermediate  $X$  are used in both cases.

One could argue, that such small spin effect present in Fig. 6 for the  $X$  case is a consequence of substantial contribution from other than VBF channel in our samples, thus pointing that our cuts may need to be refined. However, because of the weight distribution, as seen in the lower lower plot of Fig. 5, such a refinement is unlikely to be found within our tight selection, since the tail of events with spin weight exceeding 2 is very small. It seems that a better discriminating power between the  $H \rightarrow \tau\tau$  and  $X \rightarrow \tau\tau$  hypotheses can be provided by longitudinal  $\tau$ - $\tau$  spin correlation, the same as discussed already in Refs. [3, 41]. Nonetheless  $\tau$  polarization may offer (minor) help in exclusion of  $X$  hypothesis, even in the case when  $X\tau\tau$  couplings are insensitive to parity.

## 6 Summary and outlook

The main purpose of the paper was to demonstrate how the new (with respect to the ones used for sample generation) matrix elements for the production of  $\tau$ -lepton pair accompanied with two jets in  $pp$  collisions can be used

<sup>8</sup> Note that the separate treatment of  $\tau$  production from the distributions of  $\tau$  decay products enables evaluation of how important spin effects can be in experimental analyses.

<sup>9</sup> It can be used nevertheless to improve exclusion of spin-2 hypothesis.

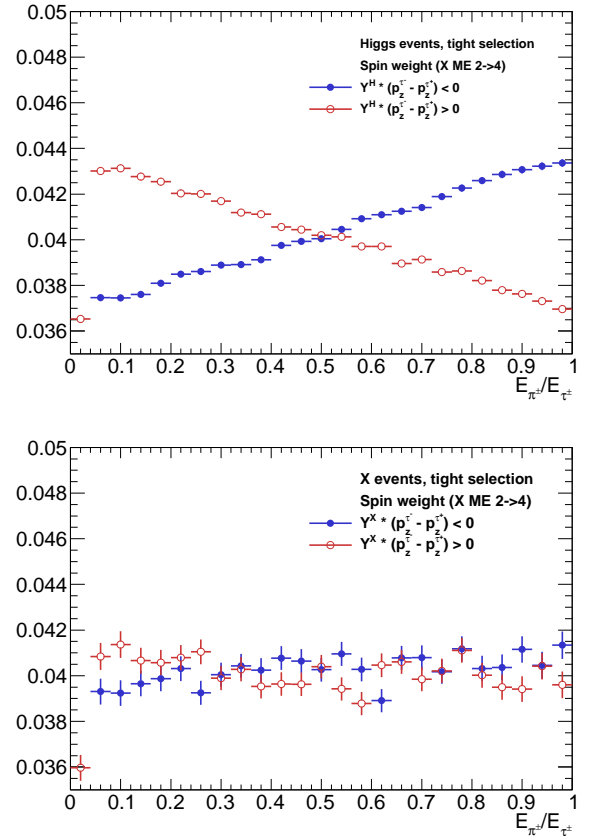


**Figure 6.** Histograms of  $E_\pi/E_\tau$  spectra, normalized to unity, for the  $H$  sample (top figure) and for the  $X$  sample (bottom figure). In all cases  $2 \rightarrow 4$  matrix elements of  $X$  exchange are used to implement spin effects. Red open circle points are for additional cut  $Y_X \cdot (p_z^{\tau^-} - p_z^{\tau^+}) > 0$  and the blue, full circle points for  $Y_X \cdot (p_z^{\tau^-} - p_z^{\tau^+}) < 0$ . Note, that because far less  $X$  events survive tight selection, statistical errors on the bottom plot are larger.

in **TauSpinner** environment to reweight events. For that purpose, the New Physics matrix element for spin-2  $X$  particle was implemented as a user example.

We have provided numerical tests of the algorithm, demonstrating that starting from the  $H$  sample (or  $X$  sample), the other one can be obtained by applying event-by-event weight calculated from the implemented matrix elements. We have also addressed possible technical difficulties and limitations in implementing the user code for matrix elements. Even though the **TauSpinner** algorithm in the case of its native and external matrix elements works similarly, technical aspects due to e.g. rounding errors and other numerical complications may differ; thus require individual attention. The density of events to be reweighted may differ from the target one significantly, resulting in a few events with weights massively larger than the ones from other regions of the phase-space.

Limitations of the algorithm, discussed in sub-section 4.3, may be observed if for example colour or spin config-

urations for original and new process play important role for the parton shower. Then, reweighting with matrix element of hard process only Eq. (2), may be too simplistic and factorization properties may need to be addressed. An effort into that direction can be found in Refs. [42, 43].

Let us stress, that the **TauSpinner** reweighting can be repeated several times on the same event to obtain multiple variants of weights, e.g. due to several variants of coupling constants, or even completely distinct  $X$  interaction forms. In our examples we have used rather small sets of non-zero couplings, see Appendix B, in part to simplify differences in distributions of  $X$  and  $H$  mediated processes. The reweighting algorithm performed better when reduced region of the phase-space was used for comparisons.

To demonstrate effects sensitive to the  $\tau$  lepton polarization we have chosen  $\tau^\pm \rightarrow \pi^\pm \nu$  decay mode as a spin analyser. Spin effects originate from the  $X$  production vertex and are embedded in complexity of the multi-body phase-space. They turn out to be rather small for our choice of the  $X\tau\tau$  couplings. Nevertheless, they may turn useful in falsifying physics hypotheses alternative to Higgs production and decay processes.

This paper completes the description of **TauSpinner** functionality, initiated in [3] for the  $2 \rightarrow 2$  matrix elements of New Physics, now also with the vector-boson-fusion  $2 \rightarrow 4$  matrix elements. It supplements examples of **TauSpinner** applications for events with two jets accompanying  $\tau$ -lepton pair production in  $pp$  collisions, discussed in [7].

## Acknowledgments

We thank Tomasz Przedziński for fruitful discussions and help with programming aspects of the **TauSpinner** code development. The work has been supported in part from funds of Polish National Science Center under decisions UMO-2014/15/B/ST2/00049, by PLGrid Infrastructure of the Academic Computer Centre CYFRONET AGH in Krakow, Poland (where majority of numerical calculations were performed) and by HARMONIA project under contract UMO-2015/18/M/ST2/00518 (2016-2019). MB, JK, ERW and ZW were supported in part by the Research Executive Agency (REA) of the European Union under the Grant Agreement PITNGA2012316704 (HiggsTools). WK was supported in part by the German DFG grant STO 876/4-1. JK thanks the CERN Theoretical Physics Department for hospitality during the final stage of this work.

## A Example with $X$ mediated processes: user installation prototype

The purpose of this Appendix is to present how the reweighting with matrix elements of  $X$  mediated process, as available in the program distribution tar-ball, can be

used. It is equally important to demonstrate how any other external matrix elements prepared by the user can be installed: the  $X$  case can serve as a prototype. The detailed instructions how the reweighting algorithm works and how it can be used for final states of  $\tau$  lepton pair and additional two jets is given already in Appendix A2 of Ref. [7]. In that paper, the non Standard Model matrix elements were not discussed.

In the case of our example of spin-2  $X$  mediated matrix elements, the command `TauSpinner::set_vbfDistrModif(SPIN2::spin2distr);` is used to set the pointer to `SPIN2::spin2distr(...,KEY)`. This can be done for the user own matrix element routines. These routines should over-load the prototype ones for the non-standard calculation.

At initialization, when command `spin2init_()` is executed the masses and coupling constants for `SPIN2::spin2distr(...,KEY)` calculation are set. Later, for every event the algorithm makes the choice for the actual matrix elements used in the weight calculation: it evaluates and pass to the user provided function its internal parameter `KEY`. The `KEY = 0, 2` corresponds to Drell-Yan like processes of the Standard Model and anomalous (user provided) matrix element. Analogously `KEY = 1, 3` is for the Higgs of the Standard Model and (user provided) matrix element for anomalous narrow resonance. The code will choose between Higgs and Drell-Yan background amplitudes on the basis of PDG identifier of the intermediate resonance found in the event record<sup>10</sup>. For `X.pdgID  $\neq$  25` it will set `KEY=0` for Standard Model (A) - that is for denominator of  $wt_{prod}^{A \rightarrow B}$  given in Eq.(2) and `KEY=2` for (B), weight numerator. For `X.pdgID = 25` it will set `KEY=1` for (A) and `KEY=3` for (B). This is why user-provided function for the matrix element calculation must have a `KEY` parameter among its arguments.

The interface assumes that the event sample is for the SM i.e. as of type (A) used in weight denominator while the user provided function is of type (B), and accordingly the weight  $wt_{prod}^{A \rightarrow B}$  is calculated. If the analyzed event sample is (as for Fig. 4) of type (B), then inverse of the weight given by Eq. (2) and calculated by **TauSpinner** should be used for reweighting.

So far, we have not discussed spin polarization and spin correlations between outgoing  $\tau$  leptons. If a generated sample features spin correlations and polarizations of  $\tau$ -leptons, then it has to be taken into account. The event weight needs to be supplemented with spin weights of the Standard Model and New Physics calculation

$$wt_{prod}^{A \rightarrow B} \rightarrow wt_{prod}^{A \rightarrow B} \cdot WT/WT0, \quad (4)$$

where `WT` and `WT0` denote usual spin weight as of Eq. (5) from Ref. [1] calculated first for (B) and then for (A). They can be obtained as shown in the extract from the code of the demonstration program.

<sup>10</sup> Let us stress that **TauSpinner** assumes that the events sample used as an input is of the Standard Model type. It determines for every event, if it is of the Higgs type, by checking if intermediate state `PDGid=25`. Otherwise, default Drell-Yan production will be assumed.

### A.1 Example of the demonstration program for $X$ mediated processes

The detailed instruction for the demonstration program is given in Appendix A4 of Ref. [7]. However, some changes were required to allow the use of  $X$  mediated amplitudes and corresponding reweighting. The distribution tar.ball [44] starting from version of Jul. 11 2017, includes necessary provisions, which are commented out. For  $X$  mediated processes they have to be activated in the following files of the directory **TAUOLA/TauSpinner/examples/example-VBF**:

- the user example program **example-VBF.cxx**,
- the prototype method **read\_particles\_for\_VBF.cxx** to read in events stored in HepMC format, prepared specifically for MadGraph5 generated events,
- the **SPIN2** directory which contains matrix elements,
- the **README** file in the **TAUOLA/TauSpinner/examples/example-VBF/SPIN2**, which contains all information for using the  $X$  matrix elements implementation which is as follow:
  - open **Makefile** in **SPIN2** directory and follow instructions there,
  - introduce a link to the **SPIN2** library into configuration of **TAUOLA/TauSpinner/examples**

To activate **SPIN2** case in **example-VBF.cxx**:

- modify **TAUOLA/TauSpinner/examples/Makefile**: uncomment lines containing string **SPIN2**,
- modify **TAUOLA/TauSpinner/examples/example-VBF/example-VBF.cxx**: again look for commented lines which contain string **spin2** or **SPIN2** and uncomment them. Note that **example-VBF.cxx** will use method **TauSpinner::set\_vbfDistrModif(SPIN2::spin2distr)**, but call on the **F77 spin2init\_()** routine for initialization of **SPIN2** library constants is necessary.
- path to **SPIN2** library has to be exported:  
`export LD_LIBRARY_PATH="/home...TAUOLA/TauSpinner/examples/example-VBF/SPIN2/lib:$LD_LIBRARY_PATH"`
- **Makefile** of **SPIN2** directory has to be executed,
- the examples of **TAUOLA/TauSpinner/examples** and **TAUOLA/TauSpinner/examples/example-VBF** with **SPIN2** library activated are ready to be compiled and linked.

For the user own external matrix elements, the scheme as of **SPIN2** should be treated as a prototype which need to be followed. The changes into the demonstration program **example-VBF.cxx** explained above provide necessary instructions. For further technical details we provide below an extract from the code.

### A.2 Extract from the code **example-VBF.cxx**.

An extract from the **TAUOLA/TauSpinner/examples/example-VBF/example-VBF.cxx** file of the distribution tar-ball. Less important, at the first reading parts, are dropped. On the other hand, code for calculation of spin weight contribution (Eq. 4) is listed.

```

//-----

// For SPIN2 code placed in directory example-VBF:
// #include "spin2distr.h" // will work once 'export SPIN2LIB=...'

//-----
/** Example function that can be used to modify/replace matrix element calculation of vbfdist present in SPIN2/ME/spin2distr.cxx */
// double spin2distr(int I1, int I2, int I3, int I4, int H1, int H2, double P[6][4], int KEY, double vbfdistr_result)

int main(int argc, char **argv) {

    if(argc<2) {
        cout<<"Usage:  "<<argv[0]<<" <input_file> [<events_limit>]" << endl;
        cout<<"Consider: "<<argv[0]<<" events-VBF.dat 10" << endl;
        exit(-1);
    }

    char *input_filename = argv[1];
    int  events_limit = 0;
    if(argc>2) events_limit = atoi(argv[2]);

    //-----
    // Initialization -----
    //-----

    // Initialize Tauola
    Tauola::initialize();
    Tauola::spin_correlation.setAll(false);

    // Initialize random numbers:
    // ##1##
    // Important when you re-decay taus: set seed for tauola-fortran random number generator RANMAR
    // int ijklin=..., int ntotin=..., int ntot2n=...; /
    // Tauola::setSeed(ijklin,ntotin,ntot2n);
    // Tauola::setSeed(time(NULL), 0, 0);

    // ##2##
    // Important when you use attributed by TauSpinner helicities
    // Replace C++ Tauola Random generator with your own (take care of seeds). Prepared method:
    // gen.SetSeed(time(NULL));
    // Tauola::setRandomGenerator( randomik );

    // Initialize LHAPDF
    // string name="MSTW2008nnlo90cl.LHgrid";
    string name="cteq6ll.LHpdf";
    // choice used for events-VBF.lhe bring tiny variation, thus it is not
    // string name="MSTW2008nlo68cl.LHgrid"; // statistically important
    LHAPDF::initPDFSetByName(name);

    // CMSENE is the center of mass energy used in PDF calculations; only if Ipp = true
    // and only for Z/gamma*
    // Ipp - true for pp collision; otherwise polarization
    // of individual taus from Z/gamma* is set to 0.0

    // Ipol - relevant for Z/gamma* decays
    // 0 - events generated without spin effects
    // 1 - events generated with all spin effects
    // 2 - events generated with spin correlations and <pol>=0
    // 3 - events generated with spin correlations and
    // polarization but missing angular dependence of <pol>

    // nonSM2 option- 1/0 extra term in cross section, density matrix on/off
    // nonSMN option- 1/0 extra term in cross section, for shapes only on/off

    // For definition of EW and QCD schemes see Ref. [7].

    double CMSENE = 13000.0; // 14000.0;
    bool Ipp = true;
    int Ipol = 1;
    int nonSM2 = 0;
    int nonSMN = 0;

    // Initialize TauSpinner
    initialize_spinner(Ipp, Ipol, nonSM2, nonSMN, CMSENE);

    int ref=1; // EW scheme to be used for default vbf calculation.
    int variant =1; // EW scheme to be used in optional matrix element reweighting (nonSM2=1). Then
    // for vbf calculation, declared above prototype method vbfdistrModif
    // (or user function)will be used.
    // At its disposal result of calculation with variant of EW scheme will be available.
    vbfini_(&ref,&variant);

```



```

int QCDdefault=1; // QCD scheme to be used for default vbf calculation.
int QCDvariant=1; // QCD scheme to be used in optional matrix element reweighting (nonSM2=1).
setPDF0pt(QCDdefault,QCDvariant);

// Set function that modifies/replaces Matrix Element calculation of vbf distr
// TauSpinner::set_vbfDistrModif(vbfDistrModif);

// Set function that modifies/replaces Matrix Element calculation of vbf distr with code of SPIN2
// spin2init_(&ref,&variant);
// TauSpinner::set_vbfDistrModif(SPIN2::spin2distr);

// Set function that modifies/replaces alpha_s calculation of vbf distr
// TauSpinner::set_alphasModif(alphasModif);

// Open I/O files (in our example events are taken from "events.dat")
HepMC::IO_GenEvent input_file(input_filename,std::ios::in);

if(input_file.rdstate()) {
    cout<<endl<<"ERROR: file "<<input_filename<<" not found."<<endl<<endl;
    exit(-1);
}

int events_read =0;

int events_count = 0;
double wt_sum = 0.0;

//-----
// Event loop -----
//-----
while( !input_file.rdstate() ) {
    double WT = 1.0;
    double W[2][2] = { { 0.0 } };

    SimpleParticle p1, p2, X, p3, p4, tau1, tau2;
    vector<SimpleParticle> tau1_daughters, tau2_daughters;

    int status = read_particles_for_VBF(input_file,p1,p2,X,p3,p4,tau1,tau2,tau1_daughters,tau2_daughters);
    ++events_read;

    // WARNING: meaning of status may depend on the variant of read_particles_for_VBF().
    if( status == 1 ) break; // variant A
    // if ( status == 0 ) break; // variant B
    // else if( status == 1 ) { continue;} // variant B

    // setNonSMkey(0); // to calculate spin weight of Standard Model
    // double WT0 = calculateWeightFromParticlesVBF(p3, p4, X, tau1, tau2, tau1_daughters, tau2_daughters);

    // setNonSMkey(1); // e.g. for use of SPIN2 ME and calculate all weights
    WT = calculateWeightFromParticlesVBF(p3, p4, X, tau1, tau2, tau1_daughters, tau2_daughters);

    // double WTME=getWtNonSM(); // matrix element weight
    // WTME=WTME*WT/WT0; // factor to take into account spin correlations of tau-tau pair decays
    wt_sum += WT;
    ++events_count;
    if( events_count%100 == 0 ) cout << "EVT: " << events_count << endl;
    if( events_limit && events_count >= events_limit ) break;
}

cout<<endl<<"No of events read from the file: "<<events_read<<endl;
cout<<endl<<"No of events processed for spin weight: "<<events_count<<endl;
cout<< "WT average for these processed events: "<<wt_sum/events_count<<endl;

```

## B Details of MadGraph5 initialization.

The settings and parameters for the MadGraph5 [15] generation of  $H$  and spin-2  $X$  event samples used in Section 4 are collected in the web page [16]. We remind the reader that these two generation parameter sets must be carefully matched, with the corresponding ones in the initialization of native TauSpinner (file `../TauSpinner/src/VBF/VBF_init.f`) and external matrix elements. In our example, it is the file `../TauSpinner/examples/example-VBF/SPIN2/ME/SPIN2_init.f`. A similar input consistency check will have to be performed whenever user own New Physics matrix elements are installed.

Let us recall some details how the code for matrix elements of  $X$  mediated processes were prepared. After the default (automatic) initialization with MadGraph5 settings

```
set group_subprocesses Auto
set ignore_six_quark_processes False
set loop_optimized_output True
set low_mem_multicore_nlo_generation False
set loop_color_flows False
set gauge unitary
set complex_mass_scheme False
set max_npoint_for_channel 0
import model sm
define p = g u c d s u~ c~ d~ s~
define j = g u c d s u~ c~ d~ s~
define l+ = e+ mu+
define l- = e- mu-
define vl = ve vm vt
define vl~ = ve~ vm~ vt~
```

we produced the event generation code with the sets of commands given in Table 3.

The corresponding spin-2 `param_card.dat` file contains an additional block called `spin2` for model specific couplings<sup>11</sup>.

```
Block spin2
  4 1.000000e+00 # gXtautauM
  5 1.000000e+00 # gXtautauP
  6 0.000000e+00 # gXqqM
  7 0.000000e+00 # gXqqP
  8 0.000000e+00 # gXggEven
  9 0.000000e+00 # gXggOdd
 10 1.000000e+00 # gXWWEven
 11 0.000000e+00 # gXWWOdd
 12 0.000000e+00 # gXBBEven
 13 0.000000e+00 # gXBBOdd
```

as well as a block containing information about the quantum numbers [45] of the spin 2 object.

```
Block QNUMBERS 5000002 # x
  1 0 # 3 times electric charge
  2 5 # number of spin states (2S+1)
  3 1 # colour rep (1: singlet, 3: triplet, 8: octet)
  4 0 # Particle/Antiparticle distinction (0=own anti)
```

<sup>11</sup> Of the couplings of  $X$  to gauge bosons only the CP-even ones were implemented in the SPIN2 library. They are denoted in the code with a suffix `Even` and correspond to couplings  $g_{Xii}$ ,  $i = B, W, g$ , in Eq. (3).

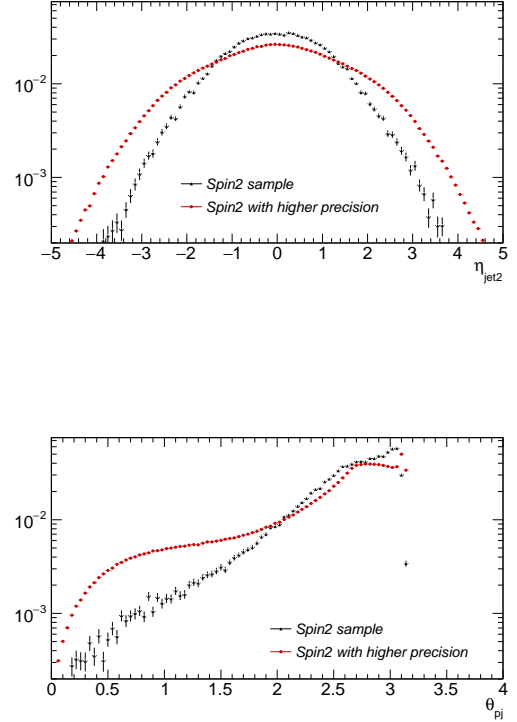


**Figure 7.** Histograms of  $\eta_{jet2}$  and  $\theta_{pj}$  distributions, normalized to unity, from MadGraph generated  $X$  samples. Black points are for the default 8 iterations used at initialization, and red (grey) points for 99 iterations.

In addition, the block containing Wolfenstein parametrization of the CKM matrix is called `ckmblock` in the Spin-2 `param_card.dat` (as opposed to name `wolfenstein` in the SM one).

The `run_card.dat` files used subsequently for generation of both  $H$  and  $X$  events are available from [16].

### B.1 Setting precision parameter of MadGraph initialization.

The weights calculated with external new matrix elements may produce a tail of rare, high weight events. This may lead to excessively large statistical errors, sometimes poorly monitored in the histograms. Their origin is from sparsely populated phase space regions in which some events receive high weight due to some resonance/-collinear configuration of the new process, see. e.g. discussion of Figs. 3 and 4 in Section 4.2 of Ref. [7].

Let us now comment on seemingly similar observations but of a fundamentally different origin. In the early steps of tests, for reweighting of  $X$  to  $H$  samples, we have encountered a mismatch between reweighted and

Higgs	X
import model sm-ckm	import model spin2_w_CKM_UFO
generate p p > j j h QED=99, h > ta+ ta-	generate p p > j j x QCD=0 QED=2 NPVV=1 NP11=1, x > ta+ ta-
output h_dir	output spin2_dir

**Table 3.** Commands to generate with the help of MadGraph5 the source code for  $H$  and  $X$  amplitudes calculation.

reference distributions generated in the gridpack mode. It turned out that the problem was related to the accuracy of samples generated by Madgraph5 based on MadEvent [46] algorithm. At MadEvent core lies the diagram enhancement method which separates the integration into a sum of integrals whose singularity structure is dictated by a single Feynman diagram topology. Each of these individual integrals, referred to as integration channel, is then integrated using an appropriate phase-space parametrisation for its underlying structure. A MadEvent run involves two steps. The first one is referred to as the survey and consists of computing cross-sections for each integration channel down to a given accuracy. Calling the `generate_events` script invokes a series of four commands: `survey`, `combine_events`, `store_events`, `create_gridpack`, in which by default `survey` should reach precision of 0.01 within 8 iterations, where the first iteration consists of 2000 points. However, with this default iteration number the required accuracy of 0.01 was not achieved and the kinematical distributions for  $X$  samples did not show a good behavior. After invoking the four commands one by one with the number of iterations in `survey`<sup>12</sup> increased to 99, the reweighted distributions were matching the reference ones (as is the case of Figs. 3 and 4). One can see in Fig. 7, that the requirement for precision for chosen distributions  $\eta_{jet2}$  and  $\theta_{pj}$  turned out to be particularly demanding.

## References

1. Z. Czyżula, T. Przedzinski and Z. Was, *TauSpinner Program for Studies on Spin Effect in tau Production at the LHC*, *Eur. Phys. J.* **C72** (2012) 1988, [1201.0117].
2. ATLAS collaboration, G. Aad et al., *Measurement of the WW cross section in  $\sqrt{s} = 7$  TeV pp collisions with the ATLAS detector and limits on anomalous gauge couplings*, *Phys. Lett.* **B712** (2012) 289–308, [1203.6232].
3. S. Banerjee, J. Kalinowski, W. Kotlarski, T. Przedzinski and Z. Was, *Ascertaining the spin for new resonances decaying into tau+ tau- at Hadron Colliders*, *Eur. Phys. J.* **C73** (2013) 2313, [1212.2873].
4. R. Józefowicz, E. Richter-Was and Z. Was, *Potential for optimizing the Higgs boson CP measurement in  $H \rightarrow \tau\tau$  decays at the LHC including machine learning techniques*, *Phys. Rev.* **D94** (2016) 093001, [1608.02609].
5. E. Barberio, B. Le, E. Richter-Was, Z. Was, D. Zanzi and J. Zaremba, *Deep learning approach to the Higgs boson CP measurement in H to tau tau decay and associated systematics*, [1706.07983].
6. Y. LeCun, Y. Bengio and G. Hinton, *Deep learning*, *Nature* **521** (2015) 436–444.
7. J. Kalinowski, W. Kotlarski, E. Richter-Was and Z. Was, *Production of  $\tau$  lepton pairs with high  $p_T$  jets at the LHC and the TauSpinner reweighting algorithm*, *Eur. Phys. J.* **C76** (2016) 540, [1604.00964]. See also M. Bahmani, J. Kalinowski, W. Kotlarski, E. Richter-Was and Z. Was, *Systematic of TauSpinner for  $\tau$  Pairs With Two Hard Jets and Its Recent Development*, *Acta Phys. Polon.* **B48**, 903 (2017).
8. ATLAS collaboration, G. Aad et al., *Search for neutral Higgs bosons of the minimal supersymmetric standard model in pp collisions at  $\sqrt{s} = 8$  TeV with the ATLAS detector*, *JHEP* **11** (2014) 056, [1409.6064].
9. CMS collaboration, *Search for additional neutral Higgs bosons decaying to a pair of tau leptons in pp collisions at  $\sqrt{s} = 7$  and 8 TeV*, *CMS-PAS-HIG-14-029*.
10. ATLAS collaboration, G. Aad et al., *Measurement of  $\tau$  polarization in  $W^- \rightarrow \tau\nu$  decays with the ATLAS detector in pp collisions at  $\sqrt{s} = 7$  TeV*, *Eur. Phys. J.* **C72** (2012) 2062, [1204.6720].
11. CMS collaboration, *Model independent search for Higgs boson pair production in the  $b\bar{b}\tau^+\tau^-$  final state*, *CMS-PAS-HIG-15-013*.
12. V. Cherepanov, *Measurement of the polarization of tau-leptons produced in Z decays at CMS and determination of the effective weak mixing angle*. PhD thesis, Aachen, Tech. Hochsch., 2016.
13. ATLAS collaboration, G. Aad et al., *Evidence for the Higgs-boson Yukawa coupling to tau leptons with the ATLAS detector*, *JHEP* **04** (2015) 117, [1501.04943].
14. ATLAS collaboration, G. Aad et al., *Modelling  $Z \rightarrow \tau\tau$  processes in ATLAS with  $\tau$ -embedded  $Z \rightarrow \mu\mu$  data*, *JINST* **10** (2015) P09018, [1506.05623].
15. J. Alwall, R. Frederix, S. Frixione, V. Hirschi, F. Maltoni, O. Mattelaer et al., *The automated computation of tree-level and next-to-leading order differential cross sections, and their matching to parton shower simulations*, *JHEP* **07** (2014) 079, [1405.0301].
16. M. Bahmani, J. Kalinowski, W. Kotlarski, E. Richter-Was and Z. Was. see <http://wasm.web.cern.ch/wasm/MadgraphIni.txt> and <http://wasm.web.cern.ch/wasm/MonitoringPlots.pdf> available from <http://wasm.web.cern.ch/wasm/newprojects.html>.
17. C.-W. Chiang, N. D. Christensen, G.-J. Ding and T. Han, *Discovery in Drell-Yan Processes at the LHC*, *Phys. Rev.* **D85** (2012) 015023, [1107.5830].
18. P. Artoisenet et al., *A framework for Higgs characterisation*, *JHEP* **11** (2013) 043, [1306.6464].

<sup>12</sup> The syntax of setting `survey` options can be found by invoking the `help survey` command in the `madevent` shell.

19. J. Frank, M. Rauch and D. Zeppenfeld, *Spin-2 resonances in vector-boson-fusion processes at next-to-leading order QCD*, *Phys. Rev.* **D87** (2013) 055020, [1211.3658].
20. ATLAS collaboration, G. Aad et al., *Test of CP Invariance in vector-boson fusion production of the Higgs boson using the Optimal Observable method in the ditau decay channel with the ATLAS detector*, *Eur. Phys. J.* **C76** (2016) 658, [1602.04516].
21. CMS collaboration, A. M. Sirunyan et al., *Observation of the Higgs boson decay to a pair of tau leptons*, [1708.00373].
22. G. Das, C. Degrande, V. Hirschi, F. Maltoni and H.-S. Shao, *NLO predictions for the production of a spin-two particle at the LHC*, *Phys. Lett.* **B770** (2017) 507–513, [1605.09359].
23. A. Alloul, N. D. Christensen, C. Degrande, C. Duhr and B. Fuks, *FeynRules 2.0 - A complete toolbox for tree-level phenomenology*, *Comput. Phys. Commun.* **185** (2014) 2250–2300, [1310.1921].
24. C. Degrande, C. Duhr, B. Fuks, D. Grellscheid, O. Mattelaer and T. Reiter, *UFO - The Universal FeynRules Output*, *Comput. Phys. Commun.* **183** (2012) 1201–1214, [1108.2040].
25. K. Hagiwara, J. Kanzaki, Q. Li and K. Mawatari, *HELAS and MadGraph/MadEvent with spin-2 particles*, *Eur. Phys. J.* **C56** (2008) 435–447, [0805.2554].
26. P. de Aquino, W. Link, F. Maltoni, O. Mattelaer and T. Stelzer, *omputations*, *Comput. Phys. Commun.* **183** (2012) 2254 doi:10.1016/j.cpc.2012.05.004 [arXiv:1108.2041 [hep-ph]].
27. I. Antcheva et al., *Comput. Phys. Commun.* **180**, 2499 (2009) doi:10.1016/j.cpc.2009.08.005 [arXiv:1508.07749 [physics.data-an]].
28. F. Schissler, [https://www.itp.kit.edu/vbfnlo/wiki/lib/exe/fetch.php?media=documentation:repolo\\_1.0.pdf](https://www.itp.kit.edu/vbfnlo/wiki/lib/exe/fetch.php?media=documentation:repolo_1.0.pdf)
29. S. Mrenna and P. Skands, *Phys. Rev. D* **94** (2016) no.7, 074005 doi:10.1103/PhysRevD.94.074005 [arXiv:1605.08352 [hep-ph]].
30. E. Bothmann, M. Scoenher and S. Schumann, *Eur. Phys. J. C* **76** (2016) no.11, 590 doi:10.1140/epjc/s10052-016-4430-0 [arXiv:1606.08753 [hep-ph]].
31. P. Artoisenet, V. Lemaître, F. Maltoni and O. Mattelaer, *JHEP* **1012** (2010) 068 doi:10.1007/JHEP12(2010)068 [arXiv:1007.3300 [hep-ph]].
32. G. Aad et al. [ATLAS Collaboration], *Eur. Phys. J. C* **70** (2010) 823 doi:10.1140/epjc/s10052-010-1429-9 [arXiv:1005.4568 [physics.ins-det]].
33. see e.g. <http://hepmc.web.cern.ch/hepmc>
34. M. Dobbs and J. B. Hansen, *Comput. Phys. Commun.* **134** (2001) 41. doi:10.1016/S0010-4655(00)00189-2
35. The manual can be found in [http://hepmc.web.cern.ch/hepmc/releases/HepMC2\\_user\\_manual.pdf](http://hepmc.web.cern.ch/hepmc/releases/HepMC2_user_manual.pdf).
36. J. Alwall et al., *Comput. Phys. Commun.* **176** (2007) 300 doi:10.1016/j.cpc.2006.11.010 [hep-ph/0609017].
37. G. Aad et al. [ATLAS Collaboration], *Eur. Phys. J. C* **76** (2016) no.6, 322 doi:10.1140/epjc/s10052-016-4126-5 [arXiv:1602.00988 [hep-ex]].
38. A. J. Larkoski, I. Moult and B. Nachman, arXiv:1709.04464 [hep-ph].
39. E. M. Metodiev, B. Nachman and J. Thaler, *JHEP* **1710**, 174 (2017) doi:10.1007/JHEP10(2017)174 [arXiv:1708.02949 [hep-ph]].
40. N. Davidson, G. Nanava, T. Przedzinski, E. Richter-Was and Z. Was, *Comput. Phys. Commun.* **183** (2012) 821 doi:10.1016/j.cpc.2011.12.009 [arXiv:1002.0543 [hep-ph]].
41. A. Kaczmarek, J. Piatlicki, T. Przedzinski, E. Richter-Was and Z. Was, *Acta Phys. Polon. B* **45**, no. 10, 1921 (2014) doi:10.5506/APhysPolB.45.1921 [arXiv:1402.2068 [hep-ph]].
42. E. Richter-Was and Z. Was, *Separating electroweak and strong interactions in Drell–Yan processes at LHC: leptons angular distributions and reference frames*, *Eur. Phys. J.* **C76** (2016) 473, [1605.05450].
43. E. Richter-Was and Z. Was, *W production at LHC: lepton angular distributions and reference frames for probing hard QCD*, *Eur. Phys. J.* **C77** (2017) 111, [1609.02536].
44. N. Davidson et al., 2008–2017, the up-to-date tar-ball for the source code and documentation of Tauola and TauSpinner see <http://wasm.web.cern.ch/wasm/c++.html> or <http://tauolapp.web.cern.ch>.
45. J. Alwall et al., “A Les Houches Interface for BSM Generators,” doi:10.2172/921331 arXiv:0712.3311 [hep-ph].
46. F. Maltoni and T. Stelzer, *MadEvent: Automatic event generation with MadGraph*, *JHEP* **0302** (2003) 027, [0208156].